DOI: 10.1002/cbic.200800196

Synthesis and Characterization of a Long, Rigid Photoswitchable Cross-Linker for Promoting Peptide and Protein Conformational Change

Fuzhong Zhang, Oleg Sadovski, and G. Andrew Woolley*[a]

Azobenzene-based photoswitchable compounds can be use to photocontrol a variety of biochemical systems. In some cases, their effectiveness may be limited by the size of the conformational change that the switch undergoes. To produce an azobenzene photoswitch that undergoes a large end-to-end distance change upon isomerization, we synthesized 3,3′-diazene-1,2-diylbis{6-[2-sulfonato-4-(chloroacetylamino)phenylethynyl]benzene sulfonic acid} (DDPBA). This long, rigid, water-soluble, thiol-reactive cross-linker undergoes an end-to-end distance change of ~13 Å upon isomerization. DDPBA was successfully cross-linked to peptides through cysteine side chains. The photoswitch undergoes trans-*to-*cis *photoisomerization maximally when irradiated at 400 nm, although the efficiency of production of the* cis *isomer is lower than for simpler azobenzenes. Under steady-state illumination conditions, the percentage of* cis *form produced increases as temperature increases; ~56 %* cis *is obtained at 60 °C. Thermal relaxation occurs with a half-life of approximately 75 min at room temperature. When DDPBA was attached to an α-helical peptide with two cysteine residues at* i *and* i+*14 positions, an increase in helix content was observed after photoirradiation. When cross-linked to another peptide with two cysteine residues spaced at* i *and* i+*21 positions, a decrease in helix content after* trans-*to-*cis *isomerization was observed. Due to the small percentage of* cis *form produced under the experimental conditions, the CD signal changes were small. However, the large structural change upon photoisomerization provided by this cross-linker can potentially be used to photoswitch other biochemical systems.*

Introduction

Covalent attachment of azobenzene compounds to biomolecules can be used to photoregulate biological systems. Azobenzene has been used to photoregulate peptide structures,[1–3] enzyme activities,[4–6] oligonucleotide function,[7–9] protein/DNA binding[10–12] and ion channel activities.[13–15]

A general way of using azobenzene to generate a change in biomolecular activity is to use photoisomerization to produce a conformational change in the biomolecule. When azobenzene is introduced as a covalent cross-link, the end-to-end distance change upon isomerization of the chromophore can generate such structural changes.[2,3,16,17] The degree of biomolecular structural change will, in general, depend on the magnitude of the end-to-end distance change of the azobenzene compound. For unmodified azobenzene, this distance change is approximately 3 Å.[18] In previous studies, azobenzene was cross-linked through amide,[19] amine,[20] carbamate, urea[21] and peptide bond linkers.[2,22] While these moieties extend the end-to-end distance of the photoswitch, their flexibility can also reduce the effective change in this distance upon isomerization. For example, with the amide-functionalized azobenzene, 3,3′-bis(sulfonato)-4,4′-bis(chloroacetamide)azobenzene (BSBCA), the end-to-end distance distribution was 11–15 Å for the *cis* form and 19–23 Å for the *trans* form so that a minimum end-to-end distance change of only ~4 Å is still possible.[23]

Moroder and colleagues recently introduced an azobenzene-based cross-linker bearing rigid alkyne units at each end that was successfully used to photocontrol the conformation of collagen peptide sequences.[24,25] The alkyne units significantly extend the length of the cross-linker, but the presence of sp^3-hybridized carbon atoms on either side of the alkyne can also permit flexibility that mutes end-to-end distance changes produced. Standaert and Park have also reported efforts aimed at maximizing biomolecular conformational changes by designing azobenzene-based photoswitches incorporating extended biphenyl units with a variety of substitution patterns.[17,26] While several of these compounds look very promising from examination of molecular models, their conformational effects on peptides have yet to be measured experimentally.

Herein, we report the synthesis of a long and rigid azobenzene derivative, 3,3′-diazene-1,2-diylbis{6-[2-sulfonato-4-(chloroacetylamino)phenylethynyl]benzene sulfonic acid} (DDPBA; **1**) that can be introduced into peptides and proteins by reaction with Cys side chains. We attached this photoswitch to two model α-helical peptides, and the behaviour of these cross-linked peptides was characterized.

[a] *F. Zhang, Dr. O. Sadovski, Prof. G. A. Woolley*
Department of Chemistry, University of Toronto
80 St. George Street, Toronto, ON M5S 3H6 (Canada)
Fax: (+1) 416-978-0675
E-mail: awoolley@chem.utoronto.ca

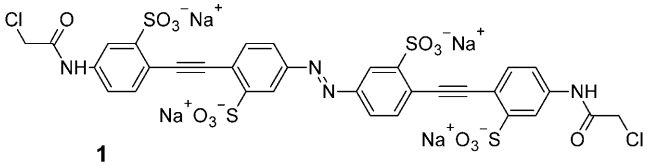

1

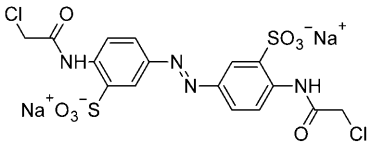

2

Results and Discussion

Cross-linker and peptide design

We chose an oligo(phenylene ethynylene) (OPE) scaffold for the design of a long, rigid linker since it provides a linear and symmetrical structure with limited conformational heterogeneity. We wished to maintain site-specific reactivity with peptides and proteins as well as water solubility. Site specificity can be achieved by reaction with Cys residues; azobenzene cross-linkers based on thiol-reactive functional groups, including iodoacetyl or chloroacetyl groups,[27,28] methanethiosulfonates[20] and alkyl halides[25,29] have been used previously. Cys residues can be easily introduced by solid-phase peptide synthesis or site-directed mutagenesis. Four sulfonate groups were incorporated to provide water solubility and inhibit hydrophobic association after cross-linking. A non-sulfonated version of the cross-linker proved only sparingly soluble in water, thus making reaction with peptides difficult.[30]

Synthesis was performed as outlined in Scheme 1. The production of **5** was adapted from the work of Temkina et al. and Ruggli and Peyer.[31,32] Reduction of **5** to the diamine compound **6** was achieved cleanly with zinc in ammonium hydroxide. Subsequent oxidation to produce the azo compound **7** yielded, in addition to the desired compound, higher oligomers as well as insoluble material. Selective monoprotection of **6** would avoid these side reactions, but would add two more synthetic steps and would require chromatographic purification of the monoprotected compound. HPLC isolation of **7** is straightforward, and the higher oligomers obtained as side-products could prove useful for other applications.

The end-to-end distance of DDPBA (**1**) in the *trans* and *cis* conformations was estimated by using molecular dynamics simulations (Figure 1). Models were built by using the program HyperChem (v.8) with methyl groups replacing the Cys β-atoms to represent the cross-linker structure after reaction with a peptide or protein. The S–S distance for the *trans* isomer ranged from 30–33 Å. In the *cis* form, the range was 13–24 Å (Figure 1 A). The most probable distance was 31.5 Å in *trans* and 18.4 Å in *cis*, a difference of ~13 Å. The minimum distance change is 6 Å, almost double that of the BSBCA cross-linker.[23]

We then designed two test peptide sequences with Cys residues spaced to match either the *trans* or *cis* form of the cross-linker. Both peptide sequences are derived from the general

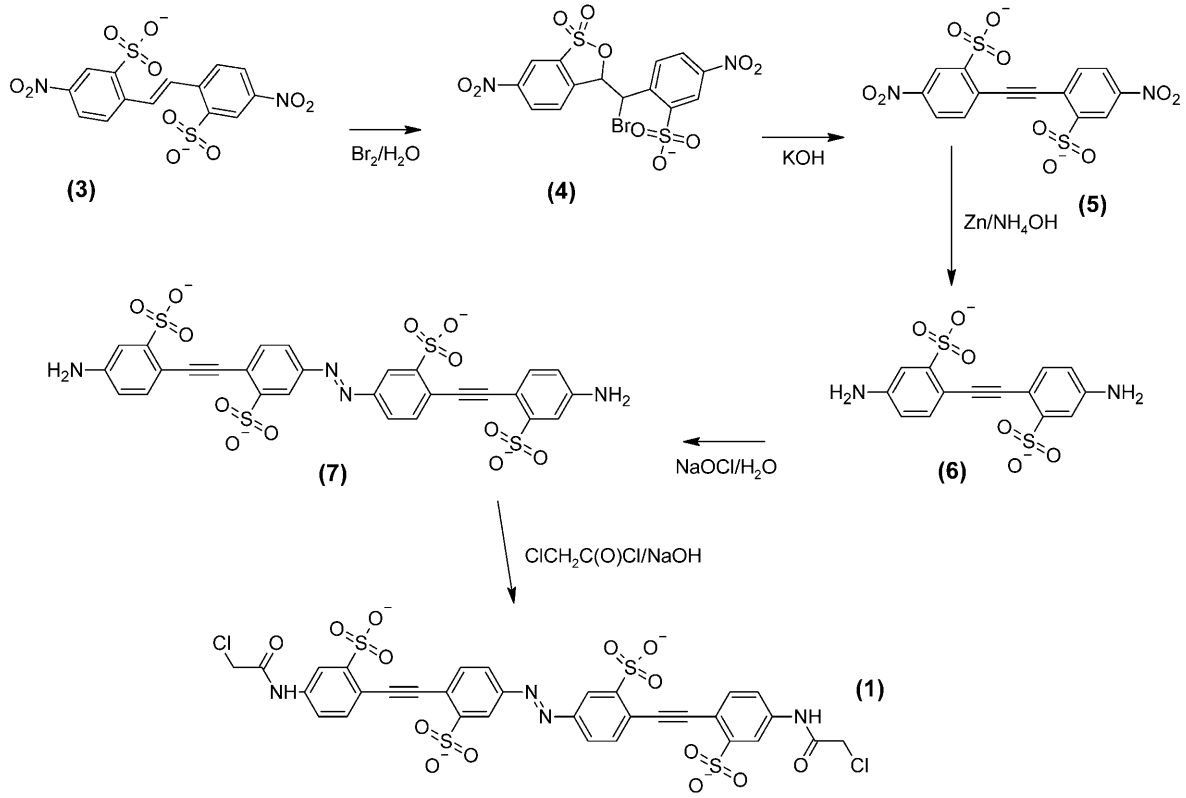

Scheme 1. Synthetic route to 3,3′-diazene-1,2-diylbis{6-[2-sulfonato-4-(chloroacetylamino)phenylethynyl]benzene sulfonic acid} (DDPBA; **1**).

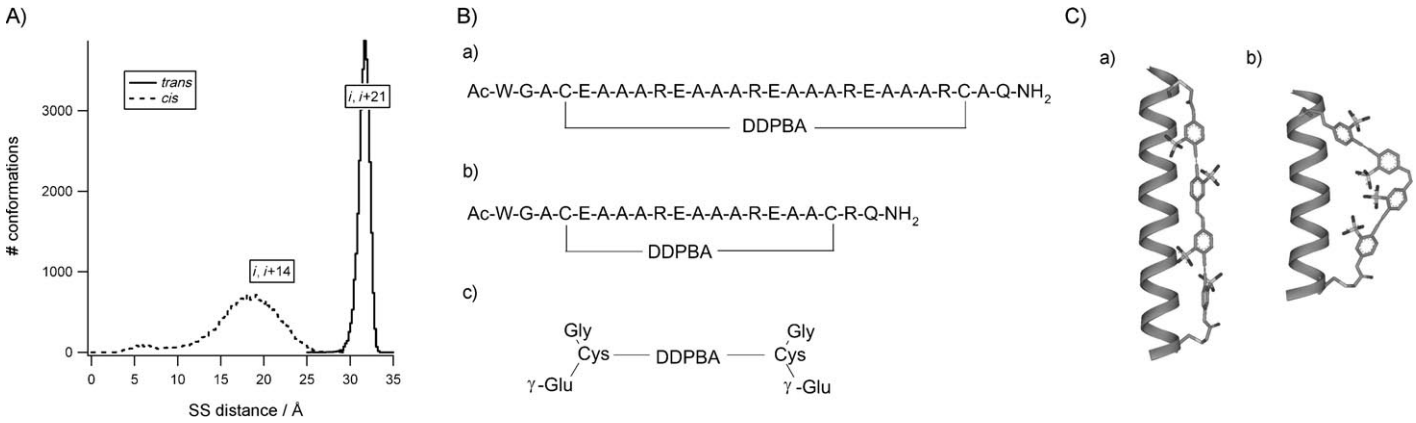

Figure 1. A) Graph of end-to-end distances for *trans* and *cis* forms of DDPBA calculated from molecular dynamics simulations. S–S spacings in ideal helical peptides with Cys residues at *i*, *i*+14 and *i*, *i*+21 are also shown. B) Primary sequences of a) XFZ21, b) XFZ14 and c) XGSH. C) Models of a) *trans* DDPBA-XFZ21 and b) *cis* DDPBA-XFZ14.

sequence Ac-(EAAAK)$_3$-A-NH$_2$ developed by Baldwin, Stellwagen et al.,[33,34] which is helical and monomeric in aqueous solution. A tryptophan with a glycine spacer was added at the N terminus of each sequence to permit concentration measurements by UV/Vis absorbance.[35] The peptide FZ21 (Figure 1B) was designed to fit to the *trans* form of the cross-linker. This peptide has Cys residues spaced at *i* and *i*+21 in the sequence so that, when the peptide adopts ideal α-helix geometry, the S atoms of the Cys side chains are spaced (32.8 ± 2) Å apart (when side-chain rotamers are considered). Peptide FZ14, with Cys residues spaced at *i* and *i*+14 positions, was designed to fit to the *cis* form of DDPBA. The S–S distance in this peptide is (21.8 ± 2) Å. These distances overlap closely with preferred *trans* and *cis* end-to-end distances of the DDPBA cross-linker, respectively. Models of each cross-linked peptide (XFZ21 in *trans* form and XFZ14 in *cis* form, where X represents cross-linked peptide) are shown in Figure 1C. DDPBA was also treated with the small tripeptide glutathione to serve as an unstructured peptide-bound control.

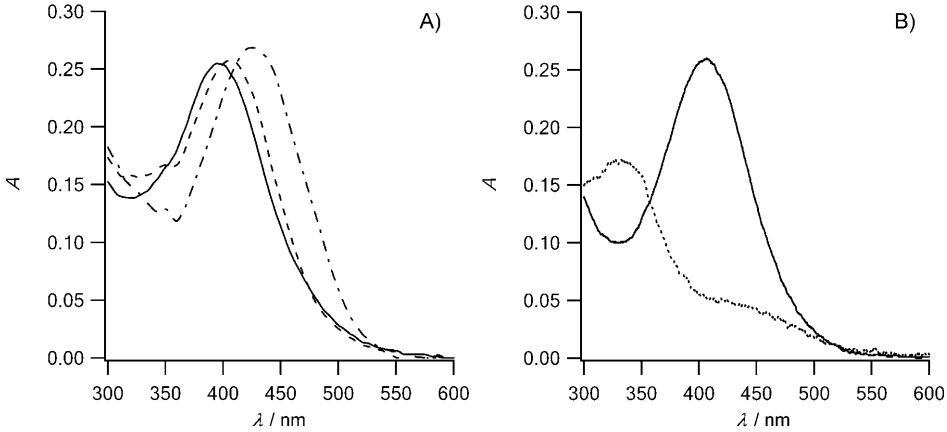

Figure 2. UV/Vis spectra of A) DDPBA in water (——), methanol (- - - -) and DMSO (–··–), and B) XFZ14 in water/40% acetonitrile; *trans* (——); *cis* (····).

UV spectra and solvent dependence

Figure 2 shows UV spectra of the *trans* form of DDPBA in water, methanol and DMSO. The maximum absorbance in water (10 mM phosphate buffer, pH 7.0) occurs at 400 nm, red shifted when compared with BSBCA cross-linker, which absorbs at 370 nm. A molar extinction coefficient of DDPBA of 25600 $M^{-1}cm^{-1}$ at 400 nm in 10 mM phosphate buffer was determined by quantitative NMR, as described in the Experimental Section. When dissolved in an organic solvent, λ_{max} shifts to longer wavelengths. In DMSO, the maximal absorbance is at 430 nm, 30 nm longer than that in aqueous solution. This solvation effect has been observed previously in amino-substituted azobenzenes,[20,36,37] but less with alkyl- and amide-substituted azobenzenes such as BSBCA. Presumably the more extended π system of DDPBA makes the UV/Vis spectrum of this molecule more sensitive to the solvation environment than with BSBCA. After DDPBA had been attached to glutathione or other peptides, the UV/Vis spectra were similar to that of free cross-linker (data not shown).

cis and *trans* isomers of peptide-linked DDPBA can be separated by reversed-phase HPLC. By coupling a diode array spectrophotometer to the HPLC system, it is possible to obtain a spectrum of the *cis* isomer before any significant thermal relaxation has occurred. The spectra of *cis* and *trans* isomers obtained in this way are shown in Figure 2B. The spectrum of the *cis* form shows a peak near 335 nm and the absorption at 400 nm decreased. The maximum wavelength of the *trans* form spectrum obtained in this way shifted to 407 nm due to the solvent effect (in 40% ACN/water), as discussed above. At 400 nm, the ratio of molar extinction coefficients between the *cis* and *trans* forms is 1:4.65 (In 40% ACN/water). This ratio was

used to estimate the percentage of *cis* form in later experiments.

Thermal isomerization kinetics

In aqueous solution, the peak in the *trans–cis* difference UV–visible spectrum is centred at 400 nm (data not shown). Accordingly, this wavelength of light was used to generate the *cis* form. We measured the thermal relaxation rate constants at several different temperatures and calculated the activation energies (Table 1). The cross-linked peptides have slightly longer relaxation half-lives than the free DDPBA at any temperature. Nevertheless, all of these photoswitchable molecules show single-exponential thermal relaxation behaviour with half-lives of approximately 75 min at room temperature (23°C). Very similar overall behaviour was found for BSBCA-linked molecules, including similar activation energies. Although the DDPBA linker is a more delocalized chromophore, a feature that can lead to enhanced thermal relaxation rates,[36,37] more atoms must move to achieve the isomerization transition state with the DDPBA linker than with the smaller BSBCA photoswitch; this perhaps accounts for a comparatively slower relaxation rate.

Table 1. Thermal relaxation half lives and activation energies.

	Thermal relaxation half-life [min]			
T [°C]	Free cross-linker	XGSH	XFZ14	XFZ21
20	75.6 ± 0.8	116 ± 2	159 ± 3	102 ± 2
30	31.5 ± 0.2	38.2 ± 0.2	53.9 ± 0.2	37.2 ± 0.1
40	9.70 ± 0.07	14.1 ± 0.03	21.4 ± 0.08	13.4 ± 0.05
50	5.85 ± 0.03	5.36 ± 0.08	7.59 ± 0.05	5.06 ± 0.02
60	2.43 ± 0.01	2.17 ± 0.01	3.94 ± 0.03	2.03 ± 0.01
70	1.08 ± 0.04	0.89 ± 0.01	1.39 ± 0.02	1.07 ± 0.01
Activation energy [kcal mol^{-1}]	16.8 ± 0.1	19.4 ± 0.2	18.6 ± 0.2	18.6 ± 0.1

Photoisomerization and the photostationary state

Upon irradiation of DDPBA at 400 nm, the spectrum shifts towards that of the *cis* form (cf. Figure 3A and B). We found that, under our standard experimental conditions (a Xenon lamp coupled to a monochromator), the percentage of *cis* form produced is much less for both DDPBA and its derivatives than that of BSBCA-linked peptides, despite the lamp intensity's being somewhat higher at 400 nm than at 370 nm. For example, at 20°C, under conditions in which the amount of the *cis* form produced is 87% for BSBCA,[38] only 24% *cis*-DDPBA is produced. Moreover, we found that under steady-state conditions (continuous irradiation), the percentage of *cis*-DDPBA produced increased as the temperature was increased. For example, Figure 3 shows UV spectra of XFZ14, with and without continuous irradiation at 400 nm, at different temperatures. Without 400 nm irradiation (Figure 3A), the spectra at different temperatures are nearly identical, thus indicating that the temperature dependence of the UV spectrum is minimal. However, under continuous irradiation (Figure 3B), the absorption band at 400 nm decreases as the temperature increases from 4 to 60°C. This decrease in absorbance at 400 nm indicates an increase in *cis* content of the sample and not simply a temperature dependence of the *cis* spectrum, because rapid cooling to 20°C of a sample irradiated at 60°C produces more *cis*-DDPBA than a sample irradiated at 20°C. This temperature-dependent behaviour is opposite to that of BSBCA and its derivatives; in that case the percentage of the *cis* form under continuous irradiation decreases as temperature increases.

Under constant illumination, the ratio of *cis* to *trans* isomers at the steady state is given by Equation (1):

$$\frac{[cis]}{[trans]} = \frac{k_{trans}}{k_{cis} + k_{\text{thermo}}} = \frac{\phi_{trans}\varepsilon_{trans} I F I_0}{\phi_{cis}\varepsilon_{cis} I F I_0 + k_{\text{thermo}}} \quad (1)$$

and the percentage of *cis* isomer is [Eq. (2)]:

$$cis\,\% = 100 \times \frac{\phi_{trans}\varepsilon_{trans} I F I_0}{\phi_{trans}\varepsilon_{trans} I F I_0 + \phi_{cis}\varepsilon_{cis} I F I_0 + k_{\text{thermo}}} \quad (2)$$

Here, k_{trans} is the rate constant for *trans*-to-*cis* photoisomerization, k_{cis} is the rate constant for *cis*-to-*trans* photoisomerization and k_{thermo} is the rate constant for *cis*-to-*trans* thermal isomerization. I_o is the light intensity, F is the photokinetic factor, ϕ_{trans} and ϕ_{cis} represent the quantum yields for *trans*-to-*cis* and *cis*-to-*trans* photoisomerization, respectively, ε_{trans} and ε_{cis} repre-

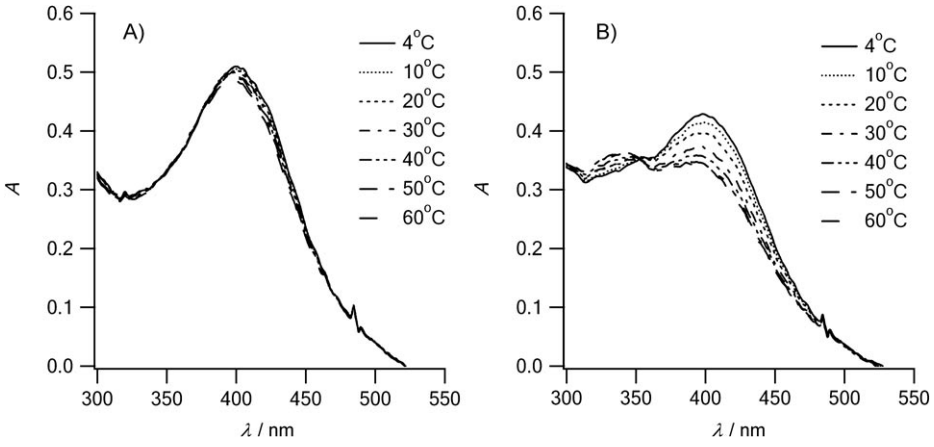

Figure 3. A) Spectra of XFZ14 without 400 nm irradiation at various temperatures. B) Spectra of the same sample obtained in the presence of continuous 400 nm irradiation. (20 μM of XFZ14 in 10 mM phosphate buffer at pH 7.0 in 1 cm pathlength cuvette.)

sent molar extinction coefficients for *trans* and *cis*, and *l* is the path length.[38]

Normally, the quantum yields ϕ_{trans} and ϕ_{cis} are relatively independent of temperature so that the primary effect of temperature is to decrease the steady-state percentage of the *cis* isomer by increasing the rate constant for thermal *cis*-to-*trans* isomerization. This decreased *cis* percentage with increased temperature is observed for BSBCA derivatives. However, with DDPBA derivatives (for example, XFZ14 (Figure 3)), although increasing the temperature from 10 to 60°C increases the rate constant for *cis*-to-*trans* thermal relaxation by 120-fold (Table 1), an increased *cis* percentage is observed at 60°C (Figure 3). This result suggests that, under the conditions of Figure 3, the thermal relaxation rate is much smaller than photoisomerization rates (k_{thermo}, k_{cis} and k_{trans}), and that the ratio of ϕ_{trans} over ϕ_{cis} increases with temperature. If so, we expect the following to be observed: 1) At any fixed temperature, if the irradiation light intensity is increased, the percentage of *cis* form should increase to a maximum (the photostationary state) set by the ratio [Eq. (3)]:

$$\frac{\phi_{trans}\varepsilon_{trans}}{\phi_{trans}\varepsilon_{trans} + \phi_{cis}\varepsilon_{cis}} \quad (3)$$

and this maximum will be larger at higher temperatures. 2) If the irradiation light intensity is reduced, to the point where k_{cis} and k_{trans} are smaller than k_{thermo}, lower temperatures will produce more *cis* form because thermal relaxation is slow.

To test these predictions, we recorded UV–visible spectra of XFZ14 under steady-state conditions with different irradiation light intensities. The light intensity was varied by placing dye solutions of various concentrations in the irradiation beam (see the Experimental Section). Figure 4 shows that the percentage of *cis* form produced under different irradiation conditions matches the expectations described above (for example, when the irradiation light intensity was reduced by 75%, more *cis* form was produced at 40°C than at 60°C). At 60°C, a maximum of approximately 56% *cis* form could be obtained. Higher temperatures led to prohibitively fast thermal relaxation. The *cis* percentage could perhaps be increased by using a narrower excitation source centred at 400 nm such as a laser or mercury arc lamp. Irradiation of a sample with intense light at 400 nm at a high temperature (60°C) followed by rapid cooling of the sample in the dark can also be used to maximize production of the *cis* isomer.

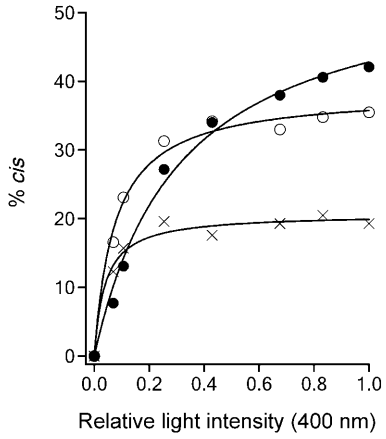

Figure 4. Percentage of *cis* form produced under steady-state illumination at 10 (×), 40 (○) and 60°C (●). Data taken at each temperature were fitted to Equation (2). (22 μM of XFZ14 in 10 mM phosphate buffer at pH 7.0.)

The relatively inefficient production of the *cis* isomer of DDPBA when compared to the BSBCA cross-linker might be due to the influence of the phenyl ethynyl units on the photochemical properties, as has been suggested recently by Tour and colleagues.[39] The size and rigidity of the DDPBA system places a requirement for rapid movement of many atoms during the short-lived excited state of the azobenzene chromophore;[40] this perhaps leads to the decreased quantum yields for isomerization, and an increase in their temperature sensitivity, as compared to the BSBCA system.

Effects of the cross-linker on peptide conformations: Circular dichroism spectra

Finally, we examined the effects of the cross-linker on peptide conformations using the test peptides FZ21 and FZ14 described above. The un-cross-linked peptides in 10 mM phosphate buffer at 20°C show 65 and 32% helix content for FZ21 and FZ14, respectively (data not shown). The *trans* (dark-adapted) form cross-linker was expected to stabilize the α-helical structure in XFZ21 and to destabilize α-helical structure in XFZ14. Destabilization was observed for XFZ14, in which only 20% helix content was observed. In XFZ21, the α-helical content was 41%, higher than that of XFZ14 but lower than un-cross-linked FZ21. If one examines a space-filling model of XFZ21, it is evident that the cross-linker must pack very closely upon the peptide surface (Figure 5). Perhaps steric interference causes some distortion of ideal helix geometry and accounts for the lower than expected helicity.

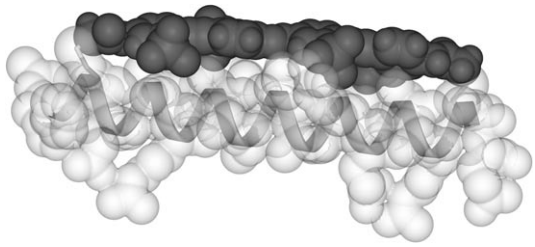

Figure 5. Model of XFZ21 showing close-packing between the DDPBA cross-linker (dark grey) and the peptide (light grey) van der Waals surfaces.

We then photoisomerized the cross-linked peptides by exposing them to 400 nm light. Approximately 15% of *cis* form was produced under our experimental conditions for the reasons discussed above. In XFZ21, a decreasing of the negative signal at 222 nm was observed upon irradiation (Figure 6A); this indicated a decrease in α-helix content consistent with the prediction that the *cis* form of the cross-linker is less compati-

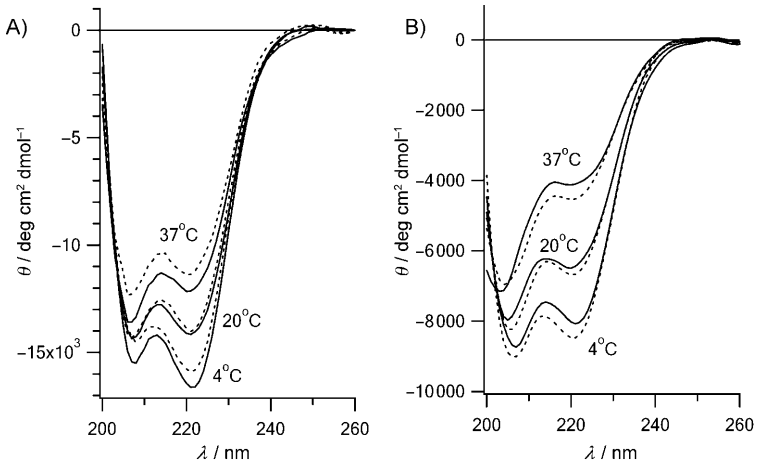

Figure 6. CD spectra of A) XFZ21 and B) XFZ14. Each peptide was scanned at 4, 20 and 37°C. Spectra after dark-adaptation are shown with solid lines. Spectra taken after irradiation (~15% *cis* isomer) are shown with dotted lines. (50 μM peptide in 10 mM phosphate buffer, pH 7.0.)

ble with FZ21 α-helical structure. For peptide XFZ14, an increase in α-helix content (corresponding to an increase in the negative signal at 222 nm) was observed after irradiation (Figure 6B). This is consistent with the prediction that the *cis* form of the cross-linker fits a folded α-helical structure of XFZ14. The overall trends of the structural changes observed with both cross-linked peptides are thus consistent with the designs. We attribute the small magnitudes of the CD changes mainly to the low yield of *cis* isomer obtained. However, it is also possible that the helix–coil cooperativity of these relatively short peptides is low, and the peptides are sufficiently flexible that they can locally distort in response to cross-linker isomerization rather than undergoing a large-scale unfolding/folding. Larger effects of photoisomerization may be seen with a target biomolecule that undergoes more rigid-body motion (for example, monomer/dimer, hinge motion).

Conclusions

We report the synthesis and characterization of a long, rigid, water-soluble, thiol-reactive cross-linker. The cross-linker can readily form intramolecular bridges in peptides and can induce conformational changes in test peptides upon isomerization. *trans*-to-*cis* photoisomerization can be accomplished by irradiating the cross-linker at 400 nm. The yield of *cis* isomer is temperature dependent, with higher yields at higher temperature (~56% at 60°C). Thermal relaxation from the *cis* to the *trans* isomer occurs with a half-life of approximately 75 min at room temperature. The large end-to-end distance changes exhibited by the cross-linker upon isomerization can in principle be used to induce large structural changes in biomolecular systems.

Experimental Section

Synthesis of the cross-linker: Compound **3** (2,2′-(*E*)-ethene-1,2-diylbis(5-nitrobenzenesulfonic acid; dinitrostilbene disulfonic acid) was purchased from City Chemical (New York, USA) and used without purification.

*1) Synthesis of 2-[bromo(6-nitro-1,1-dioxido-3H-2,1-benzoxathiol-3-yl)methyl]-5-nitrobenzenesulfonic acid (**4**)*: The sodium salt of **3** (16 g, 0.034 mol) was dissolved in water (75 mL) at 55–58°C. Then bromine (3.46 mL, 0.065 mol) was added with vigorous stirring. After 5 min, the reaction mixture was cooled to 0–5°C. The precipitate was filtered, then recrystallized from water to give 4.7 g (25%) of **4** as a yellow solid. ^{1}H NMR (400 MHz, [D$_6$]DMSO): $\delta = 6.60$ (d, $J = 9.4$ Hz, 1H), 7.73 (d, $J = 9.4$ Hz, 1H), 8.01 (d, $J = 8.7$ Hz, 1H), 8.15 (d, $J = 8.5$ Hz, 1H), 8.33 (dd, $J = 8.7$, 2.4 Hz, 1H), 8.58 (dd, $J = 8.5$ Hz, 2.4 Hz), 8.62 (d, $J = 2.4$ Hz, 1H), 8.63 ppm (d, $J = 2.4$ Hz, 1H); ^{13}C NMR (101 MHz, [D$_6$]DMSO): $\delta = 44.2$ (s, 1C), 81.6 (s, 1C), 120.4 (s, 1C), 122.7 (s, 1C), 124.9 (s, 1C), 129.1 (s, 1C), 130.5 (s, 1C), 134.3 (s, 1C), 135.3 (s, 1C), 138.0 (s, 1C), 141.6 (s, 1C), 142.6 (s, 1C), 148.3 (s, 1C), 149.8 ppm (s, 1C); HR-ESI-MS: (negative mode) $C_{14}H_8N_2O_{10}S_2Br$ calcd: 506.8809, obs: 506.8828.

*2) Synthesis of 2,2′-ethyne-1,2-diylbis(5-nitrobenzenesulfonic acid) (**5**)*: A 50% solution of potassium hydroxide (30 mL) was added to a stirred solution of **4** (9 g, 0.017 mol) in water (150 mL) at 60–70°C. The precipitate was collected and recrystallized from water to yield **5** (4.9 g, 65%) as a brown solid. ^{1}H NMR (400 MHz, D$_2$O): $\delta = 8.07$ (d, $J = 8.6$ Hz, 2H), 8.44 (dd, $J = 8.6$, 2.3 Hz, 2H), 8.75 ppm (d, $J = 2.3$ Hz, 2H); ^{13}C NMR (101 MHz, [D$_6$]DMSO): $\delta =$ 97.5 (s, 2C), 122.4 (s, 2C), 124.1 (s, 2C), 127.1 (s, 2C), 135.9 (s, 2C), 146.8 (s, 2C), 151.1 ppm (s, 2C); HR-ESI-MS: (negative mode) $C_{14}H_7N_2O_{10}S_2$ calcd: 426.9547, obs: 426.9570.

*3) Synthesis of 2,2′-ethyne-1,2-diylbis(5-aminobenzenesulfonic acid) (**6**)*: Zinc powder (Aldrich, 2 g, 0.030 mol) was added in one portion and at room temperature to a vigorously stirred solution of **5** (1 g, 2.7 mmol) in 35% ammonium hydroxide/water (150 mL). After 24 h, the solid was filtered off, and the solvent was reduced to 50 mL by rotary evaporation. The precipitate was filtered again, and the remaining liquid was mixed with silica gel, evaporated to dryness and introduced onto a silica gel column. The product was chromatographed by using ethyl acetate/methanol (7:3) as the mobile phase to give 0.58 g (67%) of **6** as a red solid. ^{1}H NMR (400 MHz, D$_2$O): $\delta = 6.9$ (dd, $J = 8.2$, 2.3 Hz, 2H), 7.3 (d, $J = 2.3$ Hz, 2H), 7.5 ppm (d, $J = 8.2$ Hz, 2H); ^{13}C NMR (101 MHz, D$_2$O): $\delta = 91.2$ (s, 2C), 109.9 (s, 2C), 114.1 (s, 2C), 118.2 (s, 2C), 135.7 (s, 2C), 143.8 (s, 2C), 147.1 ppm (s, 2C); HR-ESI-MS: (negative mode) $C_{14}H_{11}N_2O_6S_2$ calcd: 367.0064, obs: 367.0059.

*4) Synthesis of 3,3′-diazene-1,2-diylbis{6-[2-sulfonato-4-(amino)phenylethynyl]benzene sulfonic acid} (**7**)*: In a 50 mL round-bottom flask, compound **6** (1.725 g, 4.7 mmol) was suspended in distilled H$_2$O (18 mL), and the pH was adjusted to 8–9 by the addition of sodium carbonate. The solution was cooled in an ice-salt bath to −5°C, then a sodium hypochlorite solution (19 mL, 4% available chlorine (Aldrich)) was added dropwise over 6 min. The reaction mixture was left to stand at 4°C for 2–3 days. The reaction mixture was then filtered, and the mother liquor was evaporated under reduced pressure at room temperature. The solid residue (~100 mg) was dissolved in distilled H$_2$O (10 mL) with tetrabutylammonium bromide (200 mg) and injected (100–500 μL fractions) onto an HPLC column (Zorbax SB-C18, 9.4 mm × 25 cm). Eluent: solution A: 90% H$_2$O, 10% MeOH + 1 g/2.5 L tetrabutylammonium bromide, solution B: THF. Conditions: gradient from 2 to 10% solution B over 50 min (5 mL min^{-1}). The product elutes at 26–28 min and is

the most intense peak (detector at 440 nm). Excess tetrabutylammonium bromide was removed by passing the resulting solution over a cation-exchange column (SP Sephadex G25 (Sigma) equilibrated in distilled H_2O after regeneration with 0.1% NaCl, 2.5× 25 cm) to yield 0.48 g (6%) of **7** as a red solid. ^{1}H NMR (400 MHz, D_2O): $\delta = 6.9$ (dd, $J = 8.2$, 2.3 Hz, 2H), 7.3 (d, $J = 2.3$ Hz, 2H), 7.6 (d, $J = 8.2$ Hz, 2H), 7.9 (d, $J = 8.6$ Hz, 2H), 8.1 (dd, $J = 8.6$ Hz, 2.7 Hz, 2H), 8.4 ppm (d, $J = 2.7$ Hz, 2H); ^{13}C NMR (101 MHz, D_2O): $\delta = 90.7$ (s, 2C), 104.9 (s, 2C), 108.4 (s, 2C), 114.0 (s, 2C), 117.8 (s, 2C), 121.9 (s, 2C), 123.9 (s, 2C), 124.9 (s, 2C), 135.4 (s, 2C), 136.4 (s, 2C), 143.9 (s, 2C), 143.9 (s, 2C), 144.6 (s, 2C), 148.5 (s, 2C), 150.8 ppm (s, 2C); HR-ESI-MS: (negative mode) $C_{28}H_{18}N_4O_{12}S_4^{(2-)}$ calcd: 364.9907, obs: 364.9898.

*5) Synthesis of 3,3′-diazene-1,2-diylbis{6-[2-sulfonato-4-(chloroacetylamino)phenylethynyl]benzene sulfonic acid} (DDPBA) (**1**)*: NaOH (~35 μmol) was added to a solution of the tetrabutylammonium salt of **7** (15 mg, 8.5 μmol) in water to bring the pH to ~8, then chloroacetyl chloride (7 μL, ~85 μmol) was added at 0°C. After 15 min of stirring, the pH was again adjusted to pH ~8 by adding NaOH followed by chloroacetyl chloride (7 μL). After a further 5 min, the precipitate was filtered and washed with cold water several times then with THF to give **1** (9.4 mg, 60%) as a red solid. ^{1}H NMR (400 MHz, [D_6]DMSO): $\delta = 4.3$ (s, 4H), 7.6 (d, $J = 8.4$ Hz, 2H), 7.7 (dd, $J = 8.4$, 2.2 Hz, 2H), 7.8 (d, $J = 8.2$ Hz, 2H), 7.9 (dd, $J = 8.2$, 2.3 Hz, 2H), 8.1 (d, $J = 2.2$ Hz, 2H), 8.3 (d, $J = 2.3$ Hz, 2H), 11.1 ppm (s, 2H); ^{13}C NMR (101 MHz, D_2O): $\delta = 45.8$ (s, 2C), 93.0 (s, 2C), 97.8 (s, 2C), 115.6 (s, 2C), 118.6 (s, 2C), 119.8 (s, 2C), 120.9 (s, 2C), 124.4 (s, 2C), 124.8 (s, 2C), 135.5 (s, 2C), 136.1 (s, 2C), 138.7 (s, 2C), 149.2 (s, 2C), 150.7 (s, 2C), 165.7 (s, 2C), 167.4 ppm (s, 2C); HR-ESI-MS: (negative mode) $C_{32}H_{20}Cl_2N_4O_{14}S_4^{(2-)}$ calcd: 440.9623, obs: 440.9605.

Peptide synthesis and cross-linking: The peptides FZ14 (acetyl-WGACEAAAREAAAREAACRQ-amide) and FZ21 (acetyl-WGACEAAAR-EAAAREAAAREAAARCAQ-amide) were prepared by using standard Fmoc-based solid-phase peptide synthesis protocols.[20] All peptides were HPLC-purified on a Zorbax SB-C18 column with a linear gradient of 10–70% acetonitrile/water containing 0.1% trifluoroacetic acid. The compositions of the peptides were confirmed by MALDI-MS (FZ14, calcd: 2131.0 Da, obs: 2131.3 Da; FZ21, calcd: 2771.3 Da, obs: 2771.0 Da.)

Cross-linking of peptides and covalent linking to glutathione with compound **1** was preformed as follows: a final concentration of 0.5 mM peptide or glutathione was dissolved in sodium phosphate buffer (50 mM, pH 8.5) containing TCEP (10 mM). A final concentration of 2 mM of cross-linker was added, and the mixture was stirred at 37°C for 12 h. The reaction was quenched by neutralization with 1% trifluoroacetic acid. The cross-linked peptides (XFZ14 and XFZ21) and the glutathione derivative of compound **1** (XGSH) were then HPLC-purified by using the same method as described above. Yields for cross-linked peptides were between 60 and 80%. The compositions of the cross-linked peptides were checked by MALDI-MS (XFZ14, calcd: 2943.0 Da, obs: 2943.3 Da; XFZ21, calcd: 3583.0 Da, obs: 3583.2 Da. XGSH, calcd: 1426.1 Da; obs: 1426.2 Da).

UV/Vis spectra and photoisomerization: UV/Vis absorbance spectra were obtained on a Shimadzu UV-2401PC UV/Vis recording spectrophotometer or a diode array UV/Vis spectrophotometer (USB4000, Ocean Optics Int., Dunedin, FL, USA) coupled to a temperature-controlled cuvette holder (Quantum Northwest, Inc., Spokane, WA, USA) The latter arrangement was used to determine thermal relaxation rates, and steady-state spectra under UV/Vis illumination. Irradiation of the sample, at 90° to the measuring beam, was carried out with a xenon lamp (Osram 450 W XBO/2 OFR) coupled to a double monochromator with slits at 16 and 16 nm.

The molar extinction coefficient of DDPBA was determined as follows: an NMR sample with a mixture of DDPBA and a known concentration of CH_2Cl_2 in [D_6]DMSO was prepared. The concentration of DDPBA was measured by comparing the areas of methylene resonance of CH_2Cl_2 with the area of the aromatic ring signals of DDPBA. The DDPBA sample was later diluted in phosphate buffer (10 mM, pH 7.0), and UV/Vis spectra were taken to calculate the molar extinction coefficient.

Rates of thermal *cis*-to-*trans* isomerization were measured at a series of temperatures by monitoring absorbance changes at 400 nm after photoirradiation. All curves were fitted to single-exponential decay kinetics.

To obtain the UV/Vis spectrum of the *cis* state, a diode array UV/Vis spectrophotometer was used as a detector for the HPLC chromatograph. The sample was prepared by irradiating (400 nm) XFZ14 (50 μM) in phosphate buffer (10 mM, pH 7.0) at 50°C in a quartz cuvette until no further decrease in A_{400nm} was observed (~5 min). The sample was then diluted sixfold by the addition of ice-chilled water (400 μL). Immediately after dilution, the cuvette was transferred into an ice bath. The sample was injected into HPLC after it had been cooled to <10°C. *cis* and *trans* isomers were separated on a Zorbax SB-C18 column with a linear gradient 10–70% acetonitrile/water containing 0.1% trifluoroacetic acid (flow rate: 2 mL min^{-1}). The diode array UV/Vis spectrophotometer was set to take scans continually with an integration time of 600 ms for each spectrum.

For steady-state spectra, XFZ14 (22 μM) in phosphate buffer (10 mM, pH 7.0) was incubated at a series of temperatures and irradiated with the xenon lamp (400 nm) until no further absorbance change was observed. The spectra were recorded immediately (<0.2 s) after the shutter controlling the xenon lamp was closed. The irradiation light intensity was manipulated by setting a 1 cm quartz cuvette containing different concentrations of a 400 nm-absorbing dye in front of the sample cuvette to act as a filter. The 400 nm-absorbing dye was prepared by incubating dithiol-2-nitrobenzoate (DTNB) with two equivalents of β-mercaptoethanol in phosphate buffer (50 mM, pH 8.5) for 1 h. This stock solution was then diluted for use. The relative light intensity falling on the test sample was calculated from the absorbance of the filter dye solution. The wavelength distribution of the irradiation light (a narrow peak centred at 400 nm) was unaffected by the presence of the filter dye.

Circular dichroism measurements: CD spectra were recorded on an Olis RSM 1000 circular dichroism spectrophotometer with a Quantum Northwest peltier accessory. CD measurements were carried out at 4, 20 and 37°C in a 1 mm pathlength cuvette with peptide concentrations of 50 μM in phosphate buffer (10 mM, pH 7.0). Each spectrum was scanned from 260 to 195 nm with an integration time of 3 s at each wavelength. All spectra were averaged from 3 scans and baseline-corrected by using a blank consisting of phosphate buffer (10 mM, pH 7.0). To obtain CD spectra of the irradiated state, cross-linked peptide (50 μM, 400 μL) was irradiated at 50°C in a quartz UV/Vis cuvette for 5 min. The cuvette was then quickly transferred into an ice bath for cooling. From this solution, 350 μL was transferred to a CD cuvette for scanning. The remaining 50 μL sample was used to determine by UV/Vis spectrometry the percentage of the *cis* form present.

Molecular modelling: Models of *cis* and *trans* cross-linkers were built by using HyperChem (v.8, Hypercube Inc.) with the linker terminated with methyl groups to represent the β-carbon of Cys in the cross-linked peptide, and minimized by using the Amber99 force field. Restraints were added to the azo bond for the *cis* conformation (force constant 16). Molecular dynamics runs were performed in vacuo essentially as described previously[20] with a distant-dependent dielectric, and 1–4 scale factors of 0.833 for electrostatic and 0.5 for van der Waals interactions, a step size of 1 fs and 300 K as the simulation temperature. Trajectories were analyzed to verify that numerous torsion angle changes occurred for all single bonds during the course of the simulation so as to ensure that conformational space was adequately sampled. All-points histograms were then produced for the S–S distance during the full set of simulations for each isomer.

Acknowledgement

We are grateful to the Natural Sciences and Engineering Research Council of Canada (NSERC) for financial support. We thank Andrew Beharry for helpful discussions. F.Z. is supported by the Canadian Institutes of Health Research (CIHR) Protein Folding Program.

Keywords: azobenzenes · conformation changes · cross-linkers · photoswitches · rigidity

[1] O. Pieroni, A. Fissi, N. Angelini, F. Lenci, *Acc. Chem. Res.* **2001**, *34*, 9–17.
[2] C. Renner, L. Moroder, *ChemBioChem* **2006**, *7*, 868–878.
[3] G. A. Woolley, *Acc. Chem. Res.* **2005**, *38*, 486–493.
[4] M. Bose, D. Groff, J. Xie, E. Brustad, P. G. Schultz, *J. Am. Chem. Soc.* **2006**, *128*, 388–389.
[5] N. Muranaka, T. Hohsaka, M. Sisido, *FEBS Lett.* **2002**, *510*, 10–12.
[6] K. Nakayama, M. Endo, T. Majima, *Chem. Commun.* **2004**, 2386–2387.
[7] C. Dohno, S. N. Uno, K. Nakatani, *J. Am. Chem. Soc.* **2007**, *129*, 11898.
[8] X. Liang, N. Takenaka, H. Nishioka, H. Asanuma, *Chem. Asian J.* **2008**, *3*, 553–560.
[9] Y. Liu, D. Sen, *J. Mol. Biol.* **2004**, *341*, 887–892.
[10] A. M. Caamaño, M. E. Vázquez, J. Martínez-Costas, L. Castedo, J. L. Mascareñas, *Angew. Chem.* **2000**, *112*, 3234–3237; *Angew. Chem. Int. Ed.* **2000**, *39*, 3104–3107.
[11] L. Guerrero, O. S. Smart, C. J. Weston, D. C. Burns, G. A. Woolley, R. K. Allemann, *Angew. Chem.* **2005**, *117*, 7956–7960; *Angew. Chem. Int. Ed.* **2005**, *44*, 7778–7782.
[12] G. A. Woolley, A. S. Jaikaran, M. Berezovski, J. P. Calarco, S. N. Krylov, O. S. Smart, J. R. Kumita, *Biochemistry* **2006**, *45*, 6075–6084.
[13] M. Banghart, K. Borges, E. Isacoff, D. Trauner, R. H. Kramer, *Nat. Neurosci.* **2004**, *7*, 1381–1386.
[14] L. Lien, D. C. J. Jaikaran, Z. Zhang, G. A. Woolley, *J. Am. Chem. Soc.* **1996**, *118*, 12222–12223.
[15] M. Volgraf, P. Gorostiza, R. Numano, R. H. Kramer, E. Y. Isacoff, D. Trauner, *Nat. Chem. Biol.* **2006**, *2*, 47–52.
[16] A. Aemissegger, V. Krautler, W. F. van Gunsteren, D. Hilvert, *J. Am. Chem. Soc.* **2005**, *127*, 2929–2936.
[17] R. F. Standaert, S. B. Park, *J. Org. Chem.* **2006**, *71*, 7952–7966.
[18] H. Rau in *Photochemistry and Photophysics, Vol. II* (Ed.: J. F. Rabek), CRC Press, Boca Raton, **1990**, pp. 119–141.
[19] Z. Zhang, D. C. Burns, J. R. Kumita, O. S. Smart, G. A. Woolley, *Bioconjugate Chem.* **2003**, *14*, 824–829.
[20] L. Chi, O. Sadovski, G. A. Woolley, *Bioconjugate Chem.* **2006**, *17*, 670–676.
[21] N. Pozhidaeva, M. E. Cormier, A. Chaudhari, G. A. Woolley, *Bioconjugate Chem.* **2004**, *15*, 1297–1303.
[22] A. Aemissegger, D. Hilvert, *Nat. Protoc.* **2007**, *2*, 161–167.
[23] D. C. Burns, D. G. Flint, J. R. Kumita, H. J. Feldman, L. Serrano, Z. Zhang, O. S. Smart, G. A. Woolley, *Biochemistry* **2004**, *43*, 15329–15338.
[24] U. Kusebauch, S. A. Cadamuro, H. J. Musiol, M. O. Lenz, J. Wachtveitl, L. Moroder, C. Renner, *Angew. Chem.* **2006**, *118*, 7170–7173; *Angew. Chem. Int. Ed.* **2006**, *45*, 7015–7018.
[25] U. Kusebauch, S. A. Cadamuro, H. J. Musiol, L. Moroder, C. Renner, *Chem. Eur. J.* **2007**, *13*, 2966–2973.
[26] S. B. Park, R. F. Standaert, *Bioorg. Med. Chem.* **2001**, *9*, 3215–3223.
[27] D. C. Burns, F. Zhang, G. A. Woolley, *Nat. Protoc.* **2007**, *2*, 251–258.
[28] J. R. Kumita, O. S. Smart, G. A. Woolley, *Proc. Natl. Acad. Sci. USA* **2000**, *97*, 3803–3808.
[29] M. S. Vollmer, T. D. Clark, C. Steinem, M. R. Ghadiri, *Angew. Chem.* **1999**, *111*, 1703–1706; *Angew. Chem. Int. Ed.* **1999**, *38*, 1598–1601.
[30] N. Pozhidaeva, *M.Sc. Thesis*, University of Toronto (Canada), **2004**, p. 116.
[31] P. Ruggli, E. Peyer, *Helv. Chim. Acta* **1926**, *9*, 929–950.
[32] V. Temkina, G. Yaroshenko, N. Khavchenko, R. Lastovskii, *Metody Poluch. Khim. Reakt. Prep.* **1969**, *20*, 24–27.
[33] S. Marqusee, V. H. Robbins, R. L. Baldwin, *Proc. Natl. Acad. Sci. USA* **1989**, *86*, 5286–5290.
[34] G. Merutka, W. Shalongo, E. Stellwagen, *Biochemistry* **1991**, *30*, 4245–4248.
[35] A. Chakrabartty, T. Kortemme, S. Padmanabhan, R. L. Baldwin, *Biochemistry* **1993**, *32*, 5560–5565.
[36] N. Nishimura, T. Sueyoshi, H. Yamanaka, E. Imai, S. Yamamoto, S. Hasegawa, *Bull. Chem. Soc. Jpn.* **1976**, *49*, 1381–1387.
[37] R. J. W. Le Fèvre, J. Northcott, *J. Chem. Soc.* **1953**, 867–870.
[38] V. Borisenko, G. A. Woolley, *J. Photochem. Photobiol. A* **2005**, *173*, 21–28.
[39] T. Sasaki, J. M. Tour, *Org. Lett.* **2008**, *10*, 897–900.
[40] J. Bredenbeck, J. Helbing, J. R. Kumita, G. A. Woolley, P. Hamm, *Proc. Natl. Acad. Sci. USA* **2005**, *102*, 2379–2384.

Received: March 28, 2008

